Atmos. Chem. Phys. Discuss., 14, 3231–3267, 2014
www.atmos-chem-phys-discuss.net/14/3231/2014/
doi:10.5194/acpd-14-3231-2014

Atmospheric Chemistry and Physics Discussions

Estimating greenhouse gas fluxes from an agriculture-dominated landscape using multiple planetary boundary layer methods

X. Zhang[1,5], **X. Lee**[1,2], **T. J. Griffis**[3], **J. M. Baker**[4], **and W. Xiao**[2]

[1]School of Forestry and Environmental Studies, Yale University, New Haven, CT, USA
[2]Yale-NUIST Center on Atmospheric Environment, Nanjing University of Information Science and Technology, Nanjing, Jiangsu, China
[3]Department of Soil, Water, and Climate, University of Minnesota, Saint Paul, MN, USA
[4]Agricultural Research Service, USDA, Saint Paul, MN, USA
[5]Woodrow Wilson School of Public and International Affairs, Princeton University, Princeton, NJ, USA

Received: 22 November 2013 – Accepted: 14 January 2014 – Published: 3 February 2014

Correspondence to: X. Zhang (xz2@princeton.edu)

Published by Copernicus Publications on behalf of the European Geosciences Union.

Abstract

Quantification of regional greenhouse gas (GHG) fluxes is essential for establishing mitigation strategies and evaluating their effectiveness. Here, we used multiple top-down approaches and multiple trace gas observations at a tall tower to estimate GHG regional fluxes and evaluate the GHG fluxes derived from bottom-up approaches. We first applied the eddy covariance, equilibrium, inverse modeling (CarbonTracker), and flux aggregation methods using three years of carbon dioxide (CO_2) measurements on a 244 m tall tower in the Upper Midwest, USA. We then applied the equilibrium method for estimating methane (CH_4) and nitrous oxide (N_2O) fluxes with one-month high-frequency CH_4 and N_2O gradient measurements on the tall tower and one-year concentration measurements on a nearby tall tower, and evaluated the uncertainties of this application. The results indicate that: (1) the flux aggregation, eddy covariance, the equilibrium method, and the CarbonTracker product all gave similar seasonal patterns of the regional CO_2 flux (10^5–10^6 km^2), but that the equilibrium method underestimated the July CO_2 flux by 52–69 %. (2) The annual budget varied among these methods from 74 to −131 g C-CO_2 m^{-2} yr^{-1}, indicating a large uncertainty in the annual CO_2 flux estimation. (3) The regional CH_4 and N_2O emissions according to a top-down method were at least six and two times higher than the emissions from a bottom-up inventory (Emission Database for Global Atmospheric Research), respectively. (4) The global warming potentials of the CH_4 and N_2O emissions were equal in magnitude to the cooling benefit of the regional CO_2 uptake. The regional GHG budget, including both biological and anthropogenic origins, is estimated at 7 ± 160 g CO_2 eq m^{-2} yr^{-1}.

1 Introduction

Even though quantifying GHG fluxes at the regional scale (10^2–10^6 km^2) is essential for coordinating GHG mitigation strategies, observations and flux information at these relevant scales are still extremely limited (e.g., Chen et al., 2008; Nisbet and Weiss,

ACPD
14, 3231–3267, 2014

2010). To fill this scale gap, some researchers build ecosystem models and aggregate the modeled flux according to land information (e.g., Desai et al., 2008; Tang et al., 2012; Xiao et al., 2008), while others use GHG concentration observations in combination with atmospheric transport models to derive the land surface flux (Lauvaux et al., 2012; Peters et al., 2007). The aggregation method is a bottom-up approach. Another bottom-up method is the IPCC national GHG inventory system (IPCC, 2006) based on emission factors and data concerning anthropogenic activities. The bottom-up applications are relatively easy to implement; however, they require independent verification, because uncertainties in land cover, anthropogenic activity, vegetation flux, and emission factors can lead to large biases (Chen et al., 2008; Levy et al., 1999). Hence, there is a strong motivation for using top-down methods to provide an independent constraint on the regional fluxes.

There are several top-down methods for estimating regional GHG fluxes, including tall-tower eddy covariance (Davis et al., 2003), the equilibrium boundary layer approach (Bakwin et al., 2004; Betts et al., 2004; Desai et al., 2010; Helliker et al., 2004), and inverse modeling (Peters et al., 2007). Each method uses different assumptions, has inherent advantages and disadvantages, and is sensitive to different parameters. Eddy covariance (EC) provides a direct measurement of the flux using measurement of the wind fluctuations and the scalar of interest. EC has been used for CO_2 flux measurement on tall towers (Davis et al., 2003; Haszpra et al., 2005), while few tall-tower flux observations of CH_4 and N_2O have been carried out due to instrument limitations (Desai et al., 2012) and the relatively large uncertainty for these measurements (20–300 % for CH_4, 30–1800 % for N_2O) (Kroon et al., 2010). Based on the mass balance in the atmospheric boundary layer, the equilibrium method assumes that the exchange at the top of the boundary layer and the exchange at the land surface are in equilibrium over periods longer than about 1 month (Betts, 2000). The largest source of uncertainty of this method lies in determining the background concentration above the boundary layer and the entrainment rate at the top of the boundary layer. Inverse modeling determines the land surface flux using atmospheric transport models that are constrained by ob-

ACPD
14, 3231–3267, 2014

served trace gas concentrations. The prior land surface flux, land surface observations, the meteorological inputs, and atmospheric transportation schemes are all important for determining the accuracy of the modeled flux (Peters et al., 2007). As a result, the deficiency in any of these four factors can limit the accuracy of the model.

In this study, we used several top-down approaches to evaluate the bottom-up fluxes of CO_2, CH_4, and N_2O for a region dominated by agriculture. The inter-comparison of multiple techniques was used to identify systematic biases of each method and constrain the overall uncertainties. We first used CO_2 to evaluate the equilibrium boundary layer method against tall-tower eddy covariance, flux aggregation, and the flux produced by an inverse model. We then applied the equilibrium method to estimate the CH_4 and N_2O fluxes. The final task was to compare the CH_4 and N_2O fluxes with EDGAR42 (European Commission, Joint Research Centre [JRC]/Netherlands Environmental Assessment Agency [PBL], Emission Database for Global Atmospheric Research [EDGAR], release version 4.2, http://edgar.jrc.ec.europa.eu, 2011), an inventory dataset used widely in atmospheric models (Jeong et al., 2012).

2 Data and methods

2.1 Research site

The boundary layer observations were made on a 244 m communication tower located at the Rosemount Research and Outreach Center, University of Minnesota, about 25 km south of Minneapolis/Saint Paul (44°41′19″ N, 93°4′22″ W). According to the US Department of Agriculture Crop Data Layer data in 2009, the landscape around the tall tower was dominated by cropland, which accounted for 40 % of the land cover within the 10 km radius of the tower and 37 % within the 600 km radius. Corn and soybean were the dominant crop species, accounting for 55 % and 38 % of the cropland, respectively. About 40 % of the land within the 600 km radius was covered by forest, grassland and pasture. The other land use was comprised of developed land, wetland,

ACPD
14, 3231–3267, 2014

and open water. The land cover pattern described here for 2009 had a smaller corn to soybean ratio than that reported by Griffis et al. (2010) for 2007. This difference was mainly attributed to more corn plantation in 2007 stimulated by increased ethanol biofuel demand.

2.2 Mixing ratio data

CO_2 mixing ratios at the 32 m, 56 m, 100 m, and 200 m heights above the ground were measured by a tunable diode laser analyzer (TDL) (model TGA 100A, Campbell Scientific Inc., Logan, UT, USA) (Griffis et al., 2010). Air at these levels was drawn down by a pump (model DOA-V502A-FB, Gast Group Inc., Benton Harbor, MI, USA) through four Synflex tubes (6.25 mm ID) at a line pressure of 60 kPa and at a flow rate of 16 $L\,min^{-1}$. The air was sampled sequentially, each for 30 s. The sampled air was dried prior to analysis using a Nafion drier and brought to a common temperature. The CO_2 measurement was calibrated for every measurement cycle against the National Oceanic and Atmospheric Administration-Earth System Research Laboratory (NOAA-ESRL) standards. The hourly precision of the CO_2 measurement was approximately 0.03 ppm.

In addition, an intensive campaign was carried out from 30 August to 25 September (DOY 243–269), 2009. During this campaign, we measured CO_2, H_2O, CH_4, and N_2O mixing ratios at the 200 m and 3 m height on the tower. Air was drawn from these heights at a flow rate of 1.3 $L\,min^{-1}$ and 0.9 $L\,min^{-1}$, respectively, through two Synflex tubes (6.25 mm ID). A portion (0.6 $L\,min^{-1}$) of this flow was delivered to an infrared gas analyzer (IRGA model LI-6262, LI-COR, Lincoln, NE, USA) for CO_2 and H_2O mixing ratio measurements, and a small amount (180 $mL\,min^{-1}$) was delivered to another TDL for CH_4 and N_2O measurements. Measurement precisions for CO_2, CH_4, and N_2O were 0.2 ppm, 1.2 ppb, and 0.5 ppb, respectively. The IRGA was manually calibrated with a standard CO_2 gas (391.03 ± 0.03 ppm) and a dew point generator (LI-610, LI-COR) at the beginning of the experiment. The accuracy of its measurement was im-

ACPD
14, 3231–3267, 2014

proved in post-field analysis by adding offsets so that its 200 m reading matched that registered by the TDL CO_2 analyzer for the same height. The TDL for N_2O and CH_4 measurement was plumbed to a four-port manifold that used a switching sequence in the order of 200 m, 3 m, calibration zero and calibration span, with 30 s spent on each port and the first 15 s after each switching omitted from the analysis. The N_2O concentration of the calibration span was traceable to a NOAA-ESRL gold standard. The CH_4 concentration of the calibration span was calibrated against a known standard provided by a local supplier and was also traceable to the NOAA-ESRL standard scale.

2.3 Eddy covariance data

A closed-path EC system installed at the height of 100 m on the tower was used to measure the CO_2 flux from 2007 to 2009 (Griffis et al., 2010). This system consisted of a 3-D sonic anemometer-thermometer (model CSAT3, Campbell Scientific Inc.) and the TDL analyzer (model TGA 100A, Campbell Scientific) for CO_2 concentration. The sample tubing was 125 m long (6.25 mm ID, Synflex), which resulted in a typical lag time of 11 s, with Reynolds numbers exceeding 3500. Fluctuations in the velocities and concentrations were recorded at 10 Hz, and a block averaging time of 60 min was used to capture the dominant flux-containing frequencies.

Further, in 2009 two closed-path eddy covariance systems were used at two 10 m towers in the middle of corn (G21) and soybean fields (G19) (Baker and Griffis, 2005) about 3 km away from the tall tower. They recorded half-hourly fluxes of CO_2 and H_2O of these fields.

2.4 Top-down flux estimation methods

2.4.1 Tall-tower eddy covariance

Briefly, the tall-tower CO_2 flux was determined as the sum of the eddy covariance term measured at the 100 m height ($\overline{w'c'}$) and the storage term between the land surface

ACPD
14, 3231–3267, 2014

and this height (F_S).

$$F_{EC} = \overline{w'c'} + F_S \quad (1)$$

Here, we assume that horizontal and vertical advection were negligible (Davis et al., 2003; Griffis et al., 2010). Wind statistics and fluxes were transformed into the planar fit coordinate system (Lee et al., 2004). Eddy fluxes were computed using the maximum covariance method with strict limits on window size based on manifold pressure and flow rates. Flux losses attributed to a combination of sensor separation, sonic path averaging, tube attenuation, and block averaging were estimated using the analytical model of Massman (2000). These losses typically ranged between 5 % and 20 %. A detailed description of the eddy covariance system and flux calculation can be found in Griffis et al. (2010).

The eddy covariance method does not perform well in stable atmospheric conditions and friction velocity (u_*) is commonly used as a quality control for such conditions (Davis et al., 2003; Goulden et al., 1996). In this study, we discarded the nighttime flux data when u_* was less than $0.10\,m\,s^{-1}$, which is a threshold often used for agricultural environments (Baker and Griffis, 2005; Griffis et al., 2005).

Large negative fluxes in the early morning have been observed at many eddy covariance tower sites, and it may lead to an overestimation of CO_2 uptake during the growing season by as much as 20 % (Anthoni et al., 1999; Davis et al., 2003; Yi et al., 2000). Davis et al. (2003) suggest that this bias is caused by horizontal and vertical advection, and it can be corrected by excluding the negative CO_2 flux that exceeds a pre-defined level. In this study, we excluded the morning (06:00 and 10:00 LST) data when the storage term was large (i.e. $F_S < -4\,\mu mol\,m^{-2}\,s^{-1}$). This storage term screening reduced the estimated CO_2 uptake during the growing season (May to September) by 18 % and is consistent with that reported in the literature (Davis et al., 2003; Yi et al., 2000).

The monthly CO_2 flux was determined by the mean of the composite diurnal variation of the CO_2 flux. In 2009, excluding the malfunctioning of the instrument, the available

ACPD
14, 3231–3267, 2014

data was 78 %. The u_* and storage term screening eliminated an additional 12 % and 2 % of the data, respectively. Instead of filling the data gaps, we estimated the monthly mean based on the diurnal composite of the valid observations.

2.4.2 Equilibrium method

The equilibrium method (EQ) provides a way to quantify regional trace gas fluxes from mixing ratio measurements in the boundary layer (Bakwin et al., 2004; Betts, 2000; Betts et al., 2004; Denmead et al., 1996; Desai, 2010; Helliker et al., 2004; Williams et al., 2011). So far, this method has been applied to CO_2 and N_2O but not to CH_4 (Griffis et al., 2013). On the assumption that horizontal advection and storage are negligible in the boundary layer budget when averaged over relatively long timescales (weeks) (Williams et al., 2011), the land surface flux (F_{Eq}) is in balance with the exchange at the top of the boundary layer, as

$$F_{Eq} = -\rho W(c_+ - c_m) \quad (2)$$

where c_+ and c_m are the mixing ratio of CO_2, CH_4 or N_2O above and within the boundary layer, respectively and ρ and W are air density and the vertical velocity, respectively, at the top of boundary layer. Here c_+ was assumed as the concentration measured at Niwot Ridge (NWR, 40°3′11″ N, 105°35′10″ W) CO, USA, the closest background site operated by NOAA (Conway et al., 1994), and c_m was the concentration measured by TDL analyzers and calibrated to the NOAA-ESRL standards. The concentrations used in the calculation were the composite diurnal variations for each month in the case of CO_2 and the diurnal composites for the intensive campaign in the case of CH_4 and N_2O. The equilibrium method was used for calculating the CO_2 flux from 2007 to 2009. However, due to availability of data, the comparison among methods is limited to the 2009 CO_2 fluxes.

ACPD
14, 3231–3267, 2014

We used the following two methods to determine ρW (Helliker et al., 2004) for the three GHGs:

$$\rho W = \frac{F_{\mathrm{w}}}{c_{\mathrm{w},+} - c_{\mathrm{w,m}}} \tag{3}$$

$$\rho W = -\frac{\Omega}{g \cdot M_{\mathrm{air}}} \tag{4}$$

where F_{w} and $c_{\mathrm{w,m}}$ are the water vapor flux and mixing ratio measured on the tall tower, respectively, $c_{w,+}$, and Ω are the water vapor mixing ratio and the pressure vertical velocity (in units of $\mathrm{Pa\,s^{-1}}$) at the 700hPa level in the NCEP/NCAR Reanalysis-2 data, g is gravitational acceleration, and M_{air} is molecular mass of dry air ($\mathrm{g\,mol^{-1}}$). In addition, for CH_4 and N_2O, we also used CO_2 as a tracer to determine ρW:

$$\rho W = \frac{F_{\mathrm{C}}}{c_{\mathrm{C},+} - c_{\mathrm{C,m}}} \tag{5}$$

where F_{C} is the CO_2 flux measured by the EC system on the tall tower, $c_{\mathrm{C},+}$ and $c_{\mathrm{C,m}}$ are the CO_2 mixing ratio measured at the NWR background site and at the 200 m level on the tall tower, respectively.

2.4.3 Inverse modeling

We used the CO_2 flux product from the global inversion model CarbonTracker 2011_oi (CT) (Peters et al., 2007 with updates documented at http://carbontracker.noaa.gov) as a reference to compare with the flux determined with the methods described above. This product provides three-hourly CO_2 fluxes from 2000–2010 at a spatial resolution of 1° by 1°, so the number of grid points within the 100 km, 200 km, 300 km, and 600 km radii of the tall tower is 2, 10, 25, 90, respectively. The inversion CO_2 flux consists of fossil fuel burning, fire, land, and ocean flux.

ACPD
14, 3231–3267, 2014

2.5 Flux aggregation (FA)

The regional trace gas flux can be estimated by aggregating sectorial and spatial fluxes using sectorial statistics and land cover information (Chen et al., 2008; Desai et al., 2008; Nisbet and Weiss, 2010; Tang et al., 2012). The total CO_2 flux from the landscape is the sum of the biological flux and anthropogenic flux. In this study, the anthropogenic flux was the prescribed fossil fuel flux in the CarbonTracker product. The biological flux was calculated by aggregating the CO_2 flux from six major land cover types within the tall tower footprint. The six land cover types are cropland (corn and soybean), forest, grassland/pasture, wetland, open water, and developed land. The cropland CO_2 flux was the weighted average of the flux measured with EC in a soybean field and a cornfield near the tall tower as described above. The forest CO_2 flux was obtained from the AmeriFlux data archive (Level 2 data) for the deciduous forest site at the University of Michigan Biological Station (UMBS), 662 km northeast of the tall tower (Curtis et al., 2005; Schmid et al., 2003). The grassland CO_2 flux was also from USIB2 AmeriFlux for Fermi Prairie, Illinois, 503 km southeast of the tower (Gomez-Casanovas et al., 2012). Each of the three land cover types was measured by EC flux towers in 2009, and showed different seasonal patterns of CO_2 flux (Fig. 1). The biological CO_2 flux from wetland, open water, and developed land was considered as negligible in this study, because these three land cover types only accounted for about 20 % of the tall tower footprint, and the reported annual CO_2 fluxes from those land cover types were not significantly different from zero or relatively small (Striegl et al., 1998; Knoll et al., 2013; Olson et al., 2013). For example, Olson et al. (2013) reported that a temperate peat land in northern Minnesota, USA was a small net sink of CO_2 in 2009 ($-26.8 \pm 18.7\,\mathrm{g\,C\text{-}CO_2\,m^{-2}\,yr^{-1}}$), only about 5 % of the CO_2 flux from cornfield, and about 10 % of the biogenic flux in the tall tower footprint. Considering the land fraction of peat land in the tall tower footprint, the CO_2 flux was estimated to be less than 1 % of the biogenic flux.

ACPD
14, 3231–3267, 2014

3 Results

3.1 Constraints on the regional CO_2 flux

The tall tower EC CO_2 flux exhibits a strong seasonal pattern (Fig. 2). From October to April, the landscape was a net source of CO_2, and the averaged efflux was $0.68 \pm 0.10\,\mu mol\,m^{-2}\,s^{-1}$ (the mean and standard deviation of the three annual values from 2007 to 2009). From May to September, the landscape was a sink of CO_2, reaching a peak uptake in July at the rate of $-3.68 \pm 0.99\,\mu mol\,m^{-2}\,s^{-1}$. There was no monthly mean data for June 2007 and June 2009 due to measurement problems. Since June is the only month that has missing CO_2 flux data for 2009, we gap-filled it according to the flux values observed in May to July 2008 and 2009. The annual cumulative flux in 2008 and 2009 was -24 and $-131\,g\,C\text{-}CO_2\,m^{-2}\,yr^{-1}$, respectively.

The fetch of the EC flux footprint is thought to be 10 (during strong convection) to 100 (during neutral or stable condition) times the measurement height (Horst and Weil, 1992; Davis et al., 2003); however, some studies also suggest that the fetch-to-measurement-height ratio is much higher than 100 when the flux is measured at a high level (e.g. higher than 20 m) (Gash, 1986; Leclerc and Thurtell, 1990). As a result, the fetch of our EC flux could range from 1 km to more than 10 km. In order to test the size of the region that our monthly averaged EC flux represents, we used the CT and FA methods to estimate the CO_2 flux for a radius up to 600 km and compared them with the EC flux. The monthly flux values from these methods for the range of radii correlated well with the EC flux ($r > 0.9$, $p < 0.001$) (Table 1), suggesting the land surface flux was relatively homogeneous and was dominated by the seasonal pattern of the biological flux. Further, to test the accuracy of the estimation, the Nash–Sutcliffe efficiency (NSE) was calculated (Nash and Sutcliffe, 1970), as

$$\mathrm{NSE} = 1 - \frac{\sum (o_i - m_i)^2}{\sum (o_i - \bar{o})^2} \quad (6)$$

ACPD
14, 3231–3267, 2014

where o_i is the EC flux and m_i is the regional mean flux from CT or FA. The summation is performed over all months and the overbar denotes the mean over these months. It is considered a very good fit when NSE > 0.75, and a good fit when 0.65 < NSE ≤ 0.75 (Moriasi et al., 2007). The results show that the EC flux agrees very well with the regional mean flux from both the CT and FA methods with a 200 km radius or larger (NSE > 0.80). Furthermore as the radius increased from 200 km to 600 km, the CT and FA fluxes did not change significantly. The CT and FA fluxes within a 100 km radius were more positive than the EC flux, mainly due to the strong local anthropogenic emission from the Minneapolis/Saint Paul urban area. Consequently, for our tall tower site, we can consider the EC flux as representing the average flux from 600 km radius around the tall tower, a typical size of the footprint of tall tower concentration measurement (10^6 km^2; Gloor et al., 2001).

We used the Stochastic Time-Inverted Lagrangian Transport model (Lin et al., 2003) to determine the footprint of our tall tower concentration measurement at the 200 m height. (This footprint represents the source area of the EQ flux calculated based on the 200 m concentration.) During September, when the intensive campaign was carried out, we released 100 air parcels hourly at the tower and transported these parcels backward for two days. The distribution of the air parcels determined the tall tower footprint. Overlaying the weighted footprint map with the land cover map, we determined the compositions of land cover types in the tower footprint as 65 % cropland, 11 % forest, 11 % grassland, 2 % wetland, 4 % open water and 6 % developed land. The aggregated flux based on the new footprint was $-1.01\,\mu mol\,m^{-2}\,s^{-1}$ for the month of September 2009. In comparison, the EC flux during the same period was $-0.93\,\mu mol\,m^{-2}\,s^{-1}$, and the FA flux with a 300 km and 600 km radius was $-1.04\,\mu mol\,m^{-2}\,s^{-1}$ and $-0.94\,\mu mol\,m^{-2}\,s^{-1}$, respectively. The results again confirm that the land cover type around the tower was relatively homogeneous at scales ranging from 200 to 600 km.

Consequently, we consider the tall-tower EC flux as a robust estimate of the regional flux and used it to evaluate the performance of the EQ method. Two CO_2 fluxes were

ACPD
14, 3231–3267, 2014

determined by EQ method for each month, one using H_2O as a tracer (F_{EH}, calculated with ρW with Eq. 3) and the other using ρW in the NCEP reanalysis data (F_{EO}, calculated with ρW with Eq. 4) (Fig. 3). Both F_{EH} and F_{EO} reproduced the seasonal pattern of the EC flux ($r > 0.85$, $p < 0.001$) but significantly underestimated the magnitude of the flux in July. The F_{EH} and F_{EO} fluxes were only 31 % and 48 % of the EC flux in July.

3.2 GHG concentration patterns

During the intensive campaign, the CO_2 mixing ratio at the height of 200 m increased from 365.2 ppm during the first five days to 406.2 ppm during the last five days (Fig. 4). The mixing ratio changed from below that at the NWR (384.4 ppm) to above that at the NWR site, indicating a transition of the landscape from a CO_2 sink to a source. This observation is consistent with the seasonal pattern in the CO_2 flux shown in Fig. 3.

The mean CH_4 mixing ratio during the observation period was 2.096 and 2.017 ppm at the heights of 3 m and 200 m, respectively. The CH_4 mixing ratio at both heights was consistently higher than the background mixing ratio at NWR (1.844 ppm), suggesting that the landscape around the tall tower was a CH_4 source.

The N_2O mixing ratio during the observation period was also higher than that at NWR. The average N_2O mixing ratio at the heights of 3 m and 200 m was 326.7 and 324.8 ppb, which were 4.0 ppb and 2.1 ppb higher than the value at NWR site (322.7 ppb), respectively, indicating that the landscape was a N_2O source during the observation period.

3.3 Regional CH_4 and N_2O fluxes

We applied the equilibrium method in estimating the regional CH_4 and N_2O fluxes during the intensive campaign. During this period ρW determined with three independent methods (using CO_2 and H_2O tracers and the NCEP reanalysis data) was $-0.09 \pm 0.02\,\mathrm{mol\,m^{-2}\,s^{-1}}$ (mean ±1 standard deviation of the three estimates). The CH_4 and N_2O fluxes were $16.0 \pm 3.1\,\mathrm{nmol\,m^{-2}\,s^{-1}}$ and $0.19 \pm 0.04\,\mathrm{nmol\,m^{-2}\,s^{-1}}$, respectively.

ACPD
14, 3231–3267, 2014

The CH_4 and N_2O concentration measurement was available only during the intensive campaign period in 2009. Here we determined annual budget by assuming that the seasonal pattern of the concentrations at our tall tower was identical to the pattern at a nearby NOAA tall tower site (WBI in Iowa) (Andrews et al., 2013a, b; Dlugokencky et al., 2013). The WBI site was chosen because it has similar land cover types in its footprint as our tall tower site (Zhang et al., 2014). It follows that the annual regional CH_4 and N_2O fluxes were $22.45 \pm 4.18\,\mathrm{nmol\,m^{-2}\,s^{-1}}$ and $0.49 \pm 0.09\,\mathrm{nmol\,m^{-2}\,s^{-1}}$, respectively. The uncertainties of the annual fluxes were the result of the uncertainties in ρW. In comparison, the annual CH_4 and N_2O fluxes at the WBI tower were $14.5\,\mathrm{nmol\,m^{-2}\,s^{-1}}$ and $0.32\,\mathrm{nmol\,m^{-2}\,s^{-1}}$ using the equilibrium method (Zhang, 2013). The impact of advection was considered as negligible since there was no prevailing wind direction throughout the year of 2009.

4 Discussion

4.1 Annual carbon dioxide flux

Determining the annual CO_2 flux at the regional scale is challenging because the flux has both diurnal and seasonal cycles and the magnitude of the annual average is substantially smaller than the seasonal and diurnal variations. For example, in 2009, the tall tower's annual average EC flux was $-0.35\,\mu\mathrm{mol\,m^{-2}\,s^{-1}}$ ($-131\,\mathrm{g\,C\text{-}CO_2\,m^{-2}\,yr^{-1}}$), while the seasonal variation was about $6\,\mu\mathrm{mol\,m^{-2}\,s^{-1}}$ and the diurnal variation during summer time was about $40\,\mu\mathrm{mol\,m^{-2}\,s^{-1}}$, about 16 and 113 times, respectively, higher than the annual average. So far, there is no single method that can directly assess the regional CO_2 flux, because for all the available methods there are periods or conditions where the underlying theory is not met or where the available data is limited to truly capture the temporal and spatial variability. A small systematic bias in the daily and monthly flux estimation, such as that caused by the data-screening and gap-filling

ACPD
14, 3231–3267, 2014

approaches, is significant for the annual average CO_2 flux, and it may result in opposite conclusions of whether the landscape is a carbon source or a sink.

A number of studies have attempted to estimate the annual CO_2 flux in the vicinity of the Upper Midwest USA (Table 2) (Davis et al., 2003; Bakwin et al., 2004; Helliker et al., 2004; Ricciuto et al., 2008). Based on EC measurements on the LEF tall tower, which is about 260 km northeast of our tall tower, Ricciuto et al. (2008) reported that the annual CO_2 flux was 120 g C-CO_2 m^{-2} yr^{-1} with a strong inter-annual variation from 1997 to 2004 (140 g C-CO_2 m^{-2} yr^{-1}). This result was similar to Davis et al.'s (2003) result, but opposite to Helliker et al.'s (2004) EC flux for 2000, the latter of which is −71 g C-CO_2 m^{-2} yr^{-1}. The major difference is that Helliker et al. (2004) did not gap-fill the data, and the reported CO_2 flux has excluded the periods when water vapor flux was not available.

Our annual CO_2 flux was calculated as the average of monthly fluxes, and the monthly fluxes were determined by the diurnal composite of available observations after u_* and storage term screening. We performed a Monte Carlo simulation to assess the uncertainty associated with missing data following Griffis et al. (2003). We randomly removed 30 % of the data for each month, and recorded the calculated monthly and annual fluxes following the same data processing procedure. By repeating this simulation 5000 times, we determined the standard deviation of annual fluxes. As a result, the uncertainty in annual CO_2 flux due to data gaps was ±31 g C – CO_2 m^{-2} yr^{-1}. In addition, the random errors in hourly averaged EC flux may also significantly affect the annual budget. Assuming a 20 % random error in hourly EC flux, the resulting uncertainties in annual flux was ±4 g C – CO_2 m^{-2} yr^{-1}, about one magnitude lower than the uncertainties from data gaps (Morgenstern et al., 2004). Considering the uncertainties from data gaps and random errors, the 2009 CO_2 budget was −131 ± 35 g C – CO_2 m^{-2} yr^{-1}, suggesting the region around tall tower was a carbon sink.

The uncertainty of the annual FA estimate was affected by the accuracy of the land cover information, the carbon flux data for each land cover type, and anthropogenic emissions. We assessed the uncertainties of the annual CO_2 flux from each land cover

ACPD
14, 3231–3267, 2014

type with the method used for tall tower EC flux (Table 2), and assume the uncertainty of anthropogenic emission was 10 % (NRC, 2010). Without considering the uncertainties in land cover information, the annual FA flux was $-130 \pm 13\,\mathrm{g\,C-CO_2\,m^{-2}\,yr^{-1}}$. The accuracy of the Crop Data Layer was 85–95 % for major crops (Boryan et al., 2011), therefore, we assume that the fraction of each land cover type has an uncertainty up to 20 %. By using a Monte Carlo simulation we estimated the uncertainty of the annual FA estimate will increase to $34\,\mathrm{g\,C-CO_2\,m^{-2}\,yr^{-1}}$. In other words, the FA annual flux ($-130 \pm 34\,\mathrm{g\,C\text{-}CO_2\,m^{-2}\,yr^{-1}}$) showed very good agreement with the EC flux in 2009.

Although the CT monthly flux tracked the seasonal pattern of the EC and FA flux, the annual CT flux was $-54\,\mathrm{g\,C\text{-}CO_2\,m^{-2}\,yr^{-1}}$, considerably lower than EC and FA annual fluxes. This indicates that the CT method performed reasonably well on reproducing the monthly fluxes, but that it systematically underestimated the annual flux compared to the other methods.

Overall, the good agreement between EC (a top-down method) and FA (a bottom-up method) provides strong evidence that the landscape around the tall tower was a carbon sink at the rate of $-131 \pm 35\,\mathrm{g\,C-CO_2\,m^{-2}\,yr^{-1}}$ in 2009.

4.2 Uncertainties in CO_2 flux from the equilibrium method

The EQ method provided good estimates of the CO_2 flux for each month except July, when the regional CO_2 flux was the most negative (strong sink) during 2009. Excluding July, the difference between the monthly EC flux and EQ flux in 2009 was $0.37 \pm 0.29\,\mu\mathrm{mol\,m^{-2}\,s^{-1}}$, only 6 % of the seasonal variation ($6\,\mu\mathrm{mol\,m^{-2}\,s^{-1}}$). If the EQ method reproduces the EC flux in July, the NSE index would improve to above 0.9, indicating a very good fit with the EC flux.

The underestimation of the EQ flux might be attributed to uncertainties in ρW or concentration difference at the top of boundary layer ($c_+ - c_m$), according to Eq. (2). In July, the ρW was $-0.17\,\mathrm{mol\,m^{-2}\,s^{-1}}$ (Eq. 3) and $-0.26\,\mathrm{mol\,m^{-2}\,s^{-1}}$ (Eq. 4) while the concentration difference was 9.03 ppm. To bring the equilibrium flux into agreement with the

ACPD
14, 3231–3267, 2014

tall-tower EC flux ($-4.82\,\mu mol\,m^{-2}\,s^{-1}$ in July 2009), ρW would have to increase to $-0.53\,mol\,m^{-2}\,s^{-1}$, which is much larger in magnitude than $-0.26 \pm 0.09\,mol\,m^{-2}\,s^{-1}$, the average July value for 2007 to 2011 obtained with the NCEP reanalysis data. The $0.09\,mol\,m^{-2}\,s^{-1}$ uncertainty in ρW (the standard deviation of July ρW from 2007 to 2011) leads to $0.81\,\mu mol\,m^{-2}\,s^{-1}$ uncertainty in the monthly flux, about 17 % of the July flux. In addition, the monthly ρW values in 2007 to 2011 period were mostly within $-0.18 \pm 0.08\,mol\,m^{-2}\,s^{-1}$, and the maximum and minimum values were -0.05 and $-0.36\,mol\,m^{-2}\,s^{-1}$. Even the most negative value in the five-year period cannot fully explain the underestimation of the EQ flux in July, indicating that the concentration difference at the top of boundary layer maybe underestimated.

Two sources of uncertainty exist in the concentration difference observed at the top of boundary layer ($c_+ - c_m$). One is the accuracy of the CO_2 measurement at 200 m level of our tall tower site and NWR background site, and the other is the assumption that those two concentrations are the same as the concentration within and above the boundary layer. The CO_2 concentration at our tall tower was calibrated with the NOAA-ESRL standard throughout the measurement, and the measurement precision was 0.03 ppm. Meanwhile, the precision at NWR site was on the order of 0.1 ppm (Helliker et al., 2004). As a result the first source of uncertainty led to about $0.04\,\mu mol\,m^{-2}\,s^{-1}$ uncertainties, which was not significant.

The second source of uncertainty potentially can lead to $1.55\,\mu mol\,m^{-2}\,s^{-1}$ uncertainties in July CO_2 flux. The averaged CO_2 concentrations in July 2009 in the nearby background sites were 380.03 ppm (Cold Bay, Alaska, US) and 383.81 ppm (Barrow, Alaska, US), both are higher than the NWR site (386.01 ppm) and the maximum difference was 5.98 ppm, indicating the CO_2 concentration at NWR site may underestimate c_+ by up to 5.98 ppm and result in $1.55\,\mu mol\,m^{-2}\,s^{-1}$ underestimation in CO_2 flux in July. Bakwin et al. (2004) adjusted the CO_2 concentration on 30 m upward by 2.5 ppm to estimate c_m in summer. Since our CO_2 concentration was measured on 200 m, a much higher level, the uncertainty in using 200 m concentration to estimate

ACPD
14, 3231–3267, 2014

c_m should be much less than 2.5 ppm. Direct measurement at the top of boundary layer is needed to evaluate these two important uncertainties.

Another more likely source for the significant underestimation in July is that horizontal advection is not negligible when the prevailing winds align with a strong spatial gradient. With a tall tower observation network, Miles et al. (2012) reported that the CO_2 gradients between our tall tower and other sites range from 0.3 to 2.1 ppm 100 km^{-1} during the growing season. The CarbonTracker 3-D CO_2 concentration product also shows large CO_2 depletion in the upper Midwest Corn Belt during the growing season due to the strong CO_2 uptake by corn plants. According to this product, the mean concentration of the 34–1274 m air layer has an averaged gradient of 0.8 ppm (100 km^{-1}) along the prevailing wind (from northwest) in July 2009 (Fig. 5). Using a mean wind speed of 5.4 m s^{-1} recorded on the tall tower and a boundary layer depth of 1000 m (Yi et al., 2001), the resulting advection flux was $-1.88\,\mu mol\,m^{-2}\,s^{-1}$, which is comparable to the bias of the equilibrium method. In comparison, the EC flux was not as sensitive to the advective influence. For instance, using the same spatial gradient data, the advection flux at the 100 m level was only $-0.02\,\mu mol\,m^{-2}\,s^{-1}$ according to the accumulated concentration below the second CarbonTracker grid level (112 m level).

Overall, the uncertainties in ρW, $(c_+ - c_m)$, and horizontal advection can potentially lead to uncertainties in the July CO_2 flux estimate on the order of 0.81, 1.55, and $-1.88\,\mu mol\,m^{-2}\,s^{-1}$ respectively, and they might be large enough to account for the discrepancy between EQ and EC methods for July 2009 and the annual 2009 flux. Direct and accurate measurements of these three terms are needed to reduce the uncertainties.

4.3 Uncertainties in the CH_4 and N_2O fluxes

Uncertainties in trace gas concentration measurements within and above the boundary layer can lead to large uncertainties in the trace gas flux estimation. The averaged CH_4 concentrations during the intensive campaign at the nearby background sites were

ACPD
14, 3231–3267, 2014

1.883 ppm (Cold Bay, Alaska, US), 1.887 ppm (Barrow, Alaska, US), and 1.842 ppm (NWR, Colorado, US). The maximum difference between NWR and the other background sites in North America was 0.045 ppm. If the measurements at these other sites were used for the concentration above the boundary layer at the tall tower site, the regional flux would decrease by up to 4.1 $nmol\,m^{-2}\,s^{-1}$, or about 30 % of the estimated EQ flux. In addition, the uncertainty in our CH_4 concentration measurement caused by uncertainties in the calibration standard was 0.055 ppm, with a resulting uncertainty in the flux of ±5.0 $nmol\,m^{-2}\,s^{-1}$. The combined uncertainty range of the CH_4 flux is 6.9–21.0 $nmol\,m^{-2}\,s^{-1}$.

The systematic bias in the trace gas measurement between our tall tower and NOAA background sites was avoided in the other two independent boundary layer methods, which depend on the relative concentration difference at 3 m and 300 m levels and the build-up (change in concentration with time) concentration at night. Here, we used these two methods, a modified Bowen ratio method (Werner et al., 2003) and a modified nocturnal boundary layer method (Kelliher et al., 2002), to calculate the nighttime CH_4 flux for comparison with the equilibrium estimate. The modified Bowen ratio method assumes that the vertical transport of a trace gas is driven by eddy diffusion and that the diffusivity is the same for all scalar quantities. The nocturnal boundary layer method uses CO_2 as a tracer and assumes that the build-up of CO_2 and CH_4 near the land surface is caused by land surface emissions. The CH_4 fluxes from these two methods were 14.8 ± 10.3 $nmol\,m^{-2}\,s^{-1}$ and 17.1 ± 9.4 $nmol\,m^{-2}\,s^{-1}$ (Zhang et al., 2013), respectively. The results confirm that the CH_4 flux from the equilibrium method (16.0 $nmol\,m^{-2}\,s^{-1}$) gave a reasonable estimation of the regional flux.

N_2O has a much more homogeneous background concentration than CH_4 and CO_2. The differences between the background sites in the Northern Hemisphere were less than 0.5 ppb during the intensive campaign. The N_2O measurements at the tall tower were calibrated against NOAA-ESRL standards and, therefore, can be compared against the NOAA background sites. The uncertainties in the background concentration will lead to a bias within 0.05 $nmol\,m^{-2}\,s^{-1}$ for the N_2O flux estimation, or 26 % of

ACPD
14, 3231–3267, 2014

the estimated N_2O flux ($0.19\,nmol\,m^{-2}\,s^{-1}$). Applying the modified Bowen ratio method and the modified nocturnal boundary layer method, we obtained a regional nighttime N_2O flux of $1.09 \pm 0.56\,nmol\,m^{-2}\,s^{-1}$ and $0.90 \pm 0.65\,nmol\,m^{-2}\,s^{-1}$, respectively, both of which were higher than the flux estimated from the equilibrium method. It is possible that EQ method underestimated regional N_2O flux because the advection was not negligible during the intensive observation period, but it is not feasible to evaluate due to scarce N_2O concentration measurement.

4.4 Climate impact of the major GHG fluxes

According to our tall tower measurement, the regional fluxes of three major greenhouse gases in 2009 were $-131 \pm 35\,g\,C\text{-}CO_2\,m^{-2}\,yr^{-1}$, $8.50 \pm 1.58\,g\,C\text{-}CH_4\,m^{-2}\,yr^{-1}$, and $0.43 \pm 0.08\,N\text{-}N_2O\,m^{-2}\,yr^{-1}$. The global warming potential (GWP) over a 100 yr time horizon for CO_2, CH_4, and N_2O was -480 ± 128, 283 ± 53, and $205 \pm 37\,g\,CO_2\,eq\,m^{-2}\,yr^{-1}$ respectively. The GWP for CO_2 was a result of anthropogenic emission ($454\,g\,CO_2\,eq\,m^{-2}\,yr^{-1}$, according to the fossil fuel emission prescribed in CarbonTracker product) and biological CO_2 uptake ($934\,g\,CO_2\,eq\,m^{-2}\,yr^{-1}$) for the region around the tall tower (Table 2). The total climate impact of the CH_4 and N_2O emission offset about 30 % and 22 % of the biological CO_2 uptake and was comparable to the anthropogenic CO_2 emission, indicating the important role of CH_4 and N_2O for the regional GHG emission portfolio.

Considering all three major GHG fluxes, the landscape around the tall tower had a near neutral impact on the climate in 2009 ($7 \pm 160\,g\,CO_2\,eq\,m^{-2}\,yr^{-1}$). This conclusion, however, did not consider that the carbon fixed by crops will be harvested and some fraction will be transported and emitted outside of the tall tower footprint. According to West et al. (2011), the harvested biomass from our tall tower footprint is approximately $140\,g\,C - CO_2\,m^{-2}\,yr^{-1}$ ($513\,g\,CO_2\,eq\,m^{-2}\,yr^{-1}$). In other words, the tall tower footprint likely has a warming impact on the climate when all three major GHG fluxes and emission leakage are considered.

ACPD
14, 3231–3267, 2014

4.5 Comparison with the EDGAR Inventory

EDGAR is a widely used anthropogenic GHG inventory for atmospheric research, having fine spatial resolutions ($0.1^\circ \times 0.1^\circ$) (Jeong et al., 2012; Zhao et al., 2009). So far, only a few studies have evaluated it with atmospheric observations. These studies indicate that EDGAR may have significantly underestimate N_2O and CH_4 emission in North America by as much as three times (Kort et al., 2008; Miller et al., 2012).

We first compared the CH_4 and N_2O fluxes at our tall tower during the intensive campaign with EDGAR42 for the area within the 300 km radius around the tower, and found that the CH_4 flux was 5.8 times higher and the N_2O flux was 50 % higher than the EDGAR42 values. In this comparison, the EDGAR42 annual estimate was scaled to the emissions in September using its seasonal factor (1.1 for September). Another comparison was carried out on the annual time scale. The estimates of the annual CH_4 and N_2O fluxes based on the tall tower EQ measurement were 6–9 times and 2–3 times higher than the EDGAR42 annual flux respectively.

The primary reason for the lower regional CH_4 flux from EDGAR42 is because it has excluded natural sources of CH_4. Wetland is the major natural CH_4 source in this region. Although wetlands account for less than 5 % of the land around the tall tower, it is not negligible in the regional CH_4 budgeting because CH_4 emissions from wetlands can be as high as 250 $\mathrm{nmol\,m^{-2}\,s^{-1}}$ in September (Bridgham et al., 2006). EDGAR42 may have also underestimated the CH_4 emission from anthropogenic sources, because it does not account for factors such as natural gas leakage, and have low biases for the CH_4 emissions from agricultural activities (Mays et al., 2009; Wunch et al., 2009; Ussiri et al., 2009).

We hypothesize that the lower N_2O flux in the EDGAR42 inventory is likely a result of the underestimation of anthropogenic N_2O emission, since natural sources were not significant in the region around the tall tower. A recent study on global N_2O emission from a natural ecosystems suggests soil emissions in the upper-Midwest US is mostly

ACPD
14, 3231–3267, 2014

around 0.10 kg N ha^{-1} yr^{-1} (0.01 nmol m^{-2} s^{-1}) (Zhuang et al., 2012), only 10 % of the EDGAR42 anthropogenic emission.

5 Conclusions

The regional budget of CO_2, CH_4, and N_2O for the Upper Midwest USA was quantified with multiple top-down and bottom-up approaches. The four methods for the regional CO_2 flux (tall-tower eddy covariance, CarbonTracker inverse modeling, flux aggregation, and the equilibrium boundary layer method) produced similar seasonal patterns (linear correlation of the monthly flux > 0.85, $p < 0.001$). However, discrepancies exist in the magnitude of the monthly and annual fluxes. The CarbonTracker 2009 annual flux (−54 g C-CO_2 m^{-2} yr^{-1}) was much lower in magnitude than the flux aggregation estimate (−130 ± 37 g C-CO_2 m^{-2} yr^{-1}) and that measured with eddy covariance (−131 ± 40 g C-CO_2 m^{-2} yr^{-1}). The equilibrium method significantly underestimated the July uptake by 52–69 % in comparison to eddy covariance. The underestimation cannot be fully explained by the bias in ρW or concentration difference at the top of the boundary layer, and we suggest that the large spatial gradient along the prevailing wind in July 2009 was a main contributor to the underestimation.

The CH_4 and N_2O regional fluxes estimated from equilibrium method during the intensive campaign (DOY 243–269, 2009) were 16.0±3.1 and 0.19±0.04 nmol m^{-2} s^{-1}, respectively, and were 5.8 times and 50 % higher than in the EDGAR42 inventory. The annual CH_4 and N_2O fluxes also suggest significant underestimation by the EDGAR42 inventory.

Considering the global warming potential on a 100 yr time scale, the CH_4 and N_2O emissions from the landscape were comparable to the anthropogenic CO_2. The landscape appeared to have a near neutral impact on climate when all three major GHGs were considered. Our results confirm that for this agriculture dominated landscape, climate change mitigation should include CH_4 and N_2O emissions.

ACPD
14, 3231–3267, 2014

Acknowledgements. We would like to thank the University of Minnesota UMore Park for use of the facilities, and Matt Erickson (Department of Soil, Water, and Climate, University of Minnesota) for providing technical support for the tall tower measurement. Funding was provided by USDA NIFA/2010-65112-20528, the Ministry of Education of China (grant PCSIRT), the Yale Institute for Biospheric Studies, and the Yale Center for Environmental Law & Policy Research Prize Fellowship. Measurements at the WBI tower were funded by NOAA's Climate Program Office and are part of NOAA's contributions to the North American Carbon Program. We thank Charles Stanier from the University of Iowa and his students for supporting the NOAA PFP measurements at the WBI tower. CarbonTracker CT2011_ oi results provided by NOAA ESRL, Boulder, Colorado, USA from the website at http://carbontracker.noaa.gov.

References

Andrews, A. E., Kofler, J. D., Trudeau, M. E., Williams, J. C., Neff, D. H., Masarie, K. A., Chao, D. Y., Kitzis, D. R., Novelli, P. C., Zhao, C. L., Dlugokencky, E. J., Lang, P. M., Crotwell, M. J., Fischer, M. L., Parker, M. J., Lee, J. T., Baumann, D. D., Desai, A. R., Stanier, C. O., de Wekker, S. F. J., Wolfe, D. E., Munger, J. W., and Tans, P. P.: CO_2, CO and CH_4 measurements from the NOAA Earth System Research Laboratory's Tall Tower Greenhouse Gas Observing Network: instrumentation, uncertainty analysis and recommendations for future high-accuracy greenhouse gas monitoring efforts, Atmos. Meas. Tech. Discuss., 6, 1461–1553, doi:10.5194/amtd-6-1461-2013, 2013a.

Andrews, A. E., Lang, P. M., Crotwell, A. J., Kofler, J. D.: Nitrous Oxide Dry Air Mole Fractions from the NOAA ESRL Tall Tower Network using Programmable Flask Packages (PFP), Version: 2012-09-21, 2013b.

Anthoni, P. M., Law, B. E., and Unsworth, M. H.: Carbon and water vapor exchange of an open-canopied ponderosa pine ecosystem, Agr. Forest Meteorol., 95, 151–168, doi:10.1016/s0168-1923(99)00029-5, 1999.

Baker, J. M. and Griffis, T. J.: Examining strategies to improve the carbon balance of corn/soybean agriculture using eddy covariance and mass balance techniques, Agr. Forest Meteorol., 128, 163–177, doi:10.1016/j.agrformet.2004.11.005, 2005.

ACPD
14, 3231–3267, 2014

Bakwin, P. S., Davis, K. J., Yi, C., Wofsy, S. C., Munger, J. W., Haszpra, L., and Barcza, Z.: Regional carbon dioxide fluxes from mixing ratio data, Tellus B, 56, 301–311, doi:10.1111/j.1600-0889.2004.00111.x, 2004.

Betts, A. K.: Idealized model for equilibrium boundary layer over land, J. Hydrometeorol., 1, 507–523, doi:10.1175/1525-7541(2000)001<0507:Imfebl>2.0.Co;2, 2000.

Betts, A. K., Helliker, B., and Berry, J.: Coupling between CO_2, water vapor, temperature, and radon and their fluxes in an idealized equilibrium boundary layer over land, J. Geophys. Res.-Atmos., 109, D18103, doi:10.1029/2003jd004420, 2004.

Boryan, C., Yang, Z. W., Mueller, R., and Craig, M.: Monitoring US agriculture: the US Department of Agriculture, National Agricultural Statistics Service, Cropland Data Layer Program, Geocarto Int, 26, 341–358, doi:10.1080/10106049.2011.562309, 2011.

Bridgham, S. D., Megonigal, J. P., Keller, J. K., Bliss, N. B., and Trettin, C.: The carbon balance of North American wetlands, Wetlands, 26, 889–916, doi:10.1672/0277-5212(2006)26[889:Tcbona]2.0.Co;2, 2006.

Chen, B., Chen, J. M., Mo, G., Black, A., and Worthy, D. E. J.: Comparison of regional carbon flux estimates from CO_2 concentration measurements and remote sensing based footprint integration, Global Biogeochem. Cy., 22, GB2012, doi:10.1029/2007gb003024, 2008.

Conway, T. J., Tans, P. P., Waterman, L. S., and Thoning, K. W.: Evidence for interannual variability of the carbon-cycle from the National-Oceanic-and-Atmospheric-Administration Climate-Monitoring-and-Diagnostics-Laboratory Global-Air-Sampling-Network, J. Geophys. Res.-Atmos., 99, 22831–22855, doi:10.1029/94jd01951, 1994.

Curtis, P. S., Vogel, C. S., Gough, C. M., Schmid, H. P., Su, H. B., and Bovard, B. D.: Respiratory carbon losses and the carbon-use efficiency of a northern hardwood forest, 1999–2003, New Phytol., 167, 437–455, doi:10.1111/j.1469-8137.2005.01438.x, 2005.

Davis, K. J., Bakwin, P. S., Yi, C. X., Berger, B. W., Zhao, C. L., Teclaw, R. M., and Isebrands, J. G.: The annual cycles of CO_2 and H_2O exchange over a northern mixed forest as observed from a very tall tower, Global Change Biol., 9, 1278–1293, doi:10.1046/j.1365-2486.2003.00672.x, 2003.

Denmead, O. T., Raupach, M. R., Dunin, F. X., Cleugh, H. A., and Leuning, R.: Boundary layer budgets for regional estimates of scalar fluxes, Global Change Biol., 2, 255–264, doi:10.1111/j.1365-2486.1996.tb00077.x, 1996.

ACPD
14, 3231–3267, 2014

Desai, A. R.: Climatic and phenological controls on coherent regional interannual variability of carbon dioxide flux in a heterogeneous landscape, J. Geophys. Res.-Biogeo., 115, G00J02, doi:10.1029/2010jg001423, 2010.

Desai, A. R., Noormets, A., Bolstad, P. V., Chen, J. Q., Cook, B. D., Davis, K. J., Euskirchen, E. S., Gough, C. M., Martin, J. G., Ricciuto, D. M., Schmid, H. P., Tang, J. W., and Wang, W. G.: Influence of vegetation and seasonal forcing on carbon dioxide fluxes across the Upper Midwest, USA: implications for regional scaling, Agr. Forest Meteorol., 148, 288–308, doi:10.1016/j.agrformet.2007.08.001, 2008.

Desai, A. R., Helliker, B. R., Moorcroft, P. R., Andrews, A. E., and Berry, J. A.: Climatic controls of interannual variability in regional carbon fluxes from top-down and bottom-up perspectives, J. Geophys. Res.-Biogeo., 115, G02011, doi:10.1029/2009jg001122, 2010.

Desai, A., Wang, W. G., and Cook, B. D.: Uncovering mechanisms of episodic methane sources observed by a very tall eddy covariance tower, 30th Conference on Agr. For. Meteorol./1st Conference on Atmospheric Biogeosciences, Boston, MA, US, 2012.

Dlugokencky, E., Lang, P. M., and Crotwell, A. J.: Nitrous Oxide Dry Air Mole Fractions from the NOAA ESRL Global Cooperative Air Sampling Network, Version: 2012-09-21, 2013.

Gash, J. H. C.: A note on estimating the effect of a limited fetch on micrometeorological evaporation measurements, Bound.-Lay. Meteorol., 35, 409–413, doi:10.1007/Bf00118567, 1986.

Gloor, M., Bakwin, P., Hurst, D., Lock, L., Draxler, R., and Tans, P.: What is the concentration footprint of a tall tower?, J. Geophys. Res.-Atmos., 106, 17831–17840, doi:10.1029/2001jd900021, 2001.

Gomez-Casanovas, N., Matamala, R., Cook, D. R., and Gonzalez-Meler, M. A.: Net ecosystem exchange modifies the relationship between the autotrophic and heterotrophic components of soil respiration with abiotic factors in prairie grasslands, Global Change Biol., 18, 2532–2545, doi:10.1111/J.1365-2486.2012.02721.X, 2012.

Goulden, M. L., Munger, J. W., Fan, S. M., Daube, B. C., and Wofsy, S. C.: Measurements of carbon sequestration by long-term eddy covariance: methods and a critical evaluation of accuracy, Global Change Biol., 2, 169–182, doi:10.1111/j.1365-2486.1996.tb00070.x, 1996.

Griffis, T. J., Black, T. A., Morgenstern, K., Barr, A. G., Nesic, Z., Drewitt, G. B., Gaumont-Guay, D., and McCaughey, J. H.: Ecophysiological controls on the carbon balances of three southern boreal forests, Agr. Forest Meteorol., 117, 53–71, doi:10.1016/s0168-1923(03)00023-6, 2003.

ACPD
14, 3231–3267, 2014

Griffis, T. J., Lee, X., Baker, J. M., Sargent, S. D., and King, J. Y.: Feasibility of quantifying ecosystem-atmosphere (COO)-O-18-O-16 exchange using laser spectroscopy and the flux-gradient method, Agr. Forest Meteorol., 135, 44–60, doi:10.1016/j.agrformet.2005.10.002, 2005.

Griffis, T. J., Baker, J. M., Sargent, S. D., Erickson, M., Corcoran, J., Chen, M., and Billmark, K.: Influence of C-4 vegetation on (CO_2)-C-13 discrimination and isoforcing in the Upper Midwest, US, Global Biogeochem. Cy., 24, GB4006, doi:10.1029/2009gb003768, 2010.

Griffis, T. J., Lee, X., Baker, J. M., Russelle, M. P., Zhang, X., Venterea, R., and Millet, D. B.: Reconciling the differences between top-down and bottom-up estimates of nitrous oxide emissions for the US Corn Belt, Global Biogeochem. Cy., 27, 746–754, doi:10.1002/gbc.20066, 2013.

Haszpra, L., Barcza, Z., Davis, K. J., and Tarczay, K.: Long-term tall tower carbon dioxide flux monitoring over an area of mixed vegetation, Agr. Forest Meteorol., 132, 58–77, doi:10.1016/j.agrformet.2005.07.002, 2005.

Helliker, B. R., Berry, J. A., Betts, A. K., Bakwin, P. S., Davis, K. J., Denning, A. S., Ehleringer, J. R., Miller, J. B., Butler, M. P., and Ricciuto, D. M.: Estimates of net CO_2 flux by application of equilibrium boundary layer concepts to CO_2 and water vapor measurements from a tall tower, J. Geophys. Res.-Atmos., 109, D20106, doi:10.1029/2004jd004532, 2004.

Hernandez-Ramirez, G., Hatfield, J. L., Parkin, T. B., Sauer, T. J., and Prueger, J. H.: Carbon dioxide fluxes in corn-soybean rotation in the midwestern US: inter- and intra-annual variations, and biophysical controls, Agr. Forest Meteorol., 151, 1831–1842, doi:10.1016/j.agrformet.2011.07.017, 2011.

Hollinger, S. E., Bernacchi, C. J., and Meyers, T. P.: Carbon budget of mature no-till ecosystem in North Central Region of the United States, Agr. Forest Meteorol., 130, 59–69, doi:10.1016/j.agrformet.2005.01.005, 2005.

Horst, T. W. and Weil, J. C.: Footprint estimation for scalar flux measurements in the atmospheric surface-layer, Bound.-Lay. Meteorol., 59, 279–296, doi:10.1007/Bf00119817, 1992.

IPCC: 2006 IPCC Guidelines for National Greenhouse Gas Inventories, IGES, Japan, 2006.

Jeong, S., Zhao, C., Andrews, A. E., Bianco, L., Wilczak, J. M., and Fischer, M. L.: Seasonal variation of CH_4 emissions from central California, J. Geophys. Res.-Atmos., 117, D11306, doi:10.1029/2011jd016896, 2012.

ACPD
14, 3231–3267, 2014

Kelliher, F. M., Reisinger, A. R., Martin, R. J., Harvey, M. J., Price, S. J., and Sherlock, R. R.: Measuring nitrous oxide emission rate from grazed pasture using Fourier-transform infrared spectroscopy in the nocturnal boundary layer, Agr. Forest Meteorol., 111, 29–38, doi:10.1016/S0168-1923(02)00007-2, 2002.

Knoll, L. B., Vanni, M. J., Renwick, W. H., Dittman, E. K., and Gephart, J. A.: Temperate reservoirs are large carbon sinks and small CO_2 sources: results from high-resolution carbon budgets, Global Biogeochem. Cy., 27, 52–64, doi:10.1002/Gbc.20020, 2013.

Kort, E. A., Eluszkiewicz, J., Stephens, B. B., Miller, J. B., Gerbig, C., Nehrkorn, T., Daube, B. C., Kaplan, J. O., Houweling, S., and Wofsy, S. C.: Emissions of CH_4 and N_2O over the United States and Canada based on a receptor-oriented modeling framework and COBRA-NA atmospheric observations, Geophys. Res. Lett., 35, L18808, doi:10.1029/2008gl034031, 2008.

Kroon, P. S., Hensen, A., Jonker, H. J. J., Ouwersloot, H. G., Vermeulen, A. T., and Bosveld, F. C.: Uncertainties in eddy covariance flux measurements assessed from CH_4 and N_2O observations, Agr. Forest Meteorol., 150, 806–816, 2010.

Lauvaux, T., Schuh, A. E., Uliasz, M., Richardson, S., Miles, N., Andrews, A. E., Sweeney, C., Diaz, L. I., Martins, D., Shepson, P. B., and Davis, K. J.: Constraining the CO_2 budget of the corn belt: exploring uncertainties from the assumptions in a mesoscale inverse system, Atmos. Chem. Phys., 12, 337–354, doi:10.5194/acp-12-337-2012, 2012.

Leclerc, M. Y. and Thurtell, G. W.: Footprint prediction of scalar fluxes using a Markovian analysis, Bound.-Lay. Meteorol., 52, 247–258, doi:10.1007/Bf00122089, 1990.

Lee, X. H., Massman, W., and Law, B.: Handbook of Micrometeorology: A Guide for Surface Flux Measurement and Analysis, Kluwer Acad., Norwell, Mass., 250 pp., 2004.

Levy, P. E., Grelle, A., Lindroth, A., Molder, M., Jarvis, P. G., Kruijt, B., and Moncrieff, J. B.: Regional-scale CO_2 fluxes over central Sweden by a boundary layer budget method, Agr. Forest Meteorol., 98–9, 169–180, doi:10.1016/S0168-1923(99)00096-9, 1999.

Lin, J. C., Gerbig, C., Wofsy, S. C., Andrews, A. E., Daube, B. C., Davis, K. J., and Grainger, C. A.: A near-field tool for simulating the upstream influence of atmospheric observations: The Stochastic Time-Inverted Lagrangian Transport (STILT) model, J. Geophys. Res.-Atmos., 108, 4493, doi:10.1029/2002jd003161, 2003.

Massman, W. J.: A simple method for estimating frequency response corrections for eddy covariance systems, Agr. Forest Meteorol., 104, 185–198, doi:10.1016/s0168-1923(00)00164-7, 2000.

ACPD
14, 3231–3267, 2014

Mays, K. L., Shepson, P. B., Stirm, B. H., Karion, A., Sweeney, C., and Gurney, K. R.: Aircraft-based measurements of the carbon footprint of Indianapolis, Environ. Sci. Technol., 43, 7816–7823, doi:10.1021/Es901326b, 2009.

Miles, N. L., Richardson, S. J., Davis, K. J., Lauvaux, T., Andrews, A. E., West, T. O., Bandaru, V., and Crosson, E. R.: Large amplitude spatial and temporal gradients in atmospheric boundary layer CO_2 mole fractions detected with a tower-based network in the US upper Midwest, J. Geophys. Res.-Biogeo., 117, G01019, doi:10.1029/2011jg001781, 2012.

Morgenstern, K., Black, T. A., Humphreys, E. R., Griffis, T. J., Drewitt, G. B., Cai, T. B., Nesic, Z., Spittlehouse, D. L., and Livingstone, N. J.: Sensitivity and uncertainty of the carbon balance of a Pacific Northwest Douglas-fir forest during an El Nino-La Nina cycle, Agr. Forest Meteorol., 123, 201–219, doi:10.1016/j.agrformet.2003.12.003, 2004.

Moriasi, D. N., Arnold, J. G., Van Liew, M. W., Bingner, R. L., Harmel, R. D., and Veith, T. L.: Model evaluation guidelines for systematic quantification of accuracy in watershed simulations, T. Asabe, 50, 885–900, 2007.

Nash, J. E. and Sutcliffe, J. V.: River flow forecasting through conceptual models part I – A discussion of principles, J. Hydrol., 10, 282–290, doi:10.1016/0022-1694(70)90255-6, 1970.

National Research Council: Verifying Greenhouse Gas Emissions: Methods to Support International Climate Agreements, The National Academies Press, Washington, DC, 110 pp., 2010.

Nisbet, E. and Weiss, R.: Top-down versus bottom-up, Science, 328, 1241–1243, doi:10.1126/science.1189936, 2010.

Olson, D. M., Griffis, T. J., Noormets, A., Kolka, R., and Chen, J.: Interannual, seasonal, and retrospective analysis of the methane and carbon dioxide budgets of a temperate peatland, J. Geophys. Res.-Biogeo., 118, 226–238, doi:10.1002/Jgrg.20031, 2013.

Peters, W., Jacobson, A. R., Sweeney, C., Andrews, A. E., Conway, T. J., Masarie, K., Miller, J. B., Bruhwiler, L. M. P., Petron, G., Hirsch, A. I., Worthy, D. E. J., van der Werf, G. R., Randerson, J. T., Wennberg, P. O., Krol, M. C., and Tans, P. P.: An atmospheric perspective on North American carbon dioxide exchange: CarbonTracker, P. Natl. Acad. Sci. USA, 104, 18925–18930, doi:10.1073/pnas.0708986104, 2007.

Ricciuto, D. M., Butler, M. P., Davis, K. J., Cook, B. D., Bakwin, P. S., Andrews, A., and Teclaw, R. M.: Causes of interannual variability in ecosystem-atmosphere CO_2 exchange in a northern Wisconsin forest using a Bayesian model calibration, Agr. Forest Meteorol., 148, 309–327, doi:10.1016/j.agrformet.2007.08.007, 2008.

ACPD
14, 3231–3267, 2014

Schmid, H. P., Su, H. B., Vogel, C. S., and Curtis, P. S.: Ecosystem-atmosphere exchange of carbon dioxide over a mixed hardwood forest in northern lower Michigan, J. Geophys. Res.-Atmos., 108, 4417, doi:10.1029/2002jd003011, 2003.

Striegl, R. G. and Michmerhuizen, C. M.: Hydrologic influence on methane and carbon dioxide dynamics at two north-central Minnesota lakes, Limnol. Oceanogr., 43, 1519–1529, 1998.

Suyker, A. E., Verma, S. B., and Burba, G. G.: Interannual variability in net CO_2 exchange of a native tallgrass prairie, Global Change Biol., 9, 255–265, doi:10.1046/J.1365-2486.2003.00567.X, 2003.

Tang, X. G., Wang, Z. M., Liu, D. W., Song, K. S., Jia, M. M., Dong, Z. Y., Munger, J. W., Hollinger, D. Y., Bolstad, P. V., Goldstein, A. H., Desai, A. R., Dragoni, D., and Liu, X. P.: Estimating the net ecosystem exchange for the major forests in the northern United States by integrating MODIS and AmeriFlux data, Agr. Forest Meteorol., 156, 75–84, doi:10.1016/j.agrformet.2012.01.003, 2012.

Ussiri, D. A. N., Lal, R., and Jarecki, M. K.: Nitrous oxide and methane emissions from long-term tillage under a continuous corn cropping system in Ohio, Soil Till. Res., 104, 247–255, doi:10.1016/J.Still.2009.03.001, 2009.

Werner, C., Davis, K., Bakwin, P., Yi, C. X., Hurst, D., and Lock, L.: Regional-scale measurements of CH_4 exchange from a tall tower over a mixed temperate/boreal lowland and wetland forest, Global Change Biol., 9, 1251–1261, 2003.

West, T. O., Bandaru, V., Brandt, C. C., Schuh, A. E., and Ogle, S. M.: Regional uptake and release of crop carbon in the United States, Biogeosciences, 8, 2037–2046, doi:10.5194/bg-8-2037-2011, 2011.

Williams, I. N., Riley, W. J., Torn, M. S., Berry, J. A., and Biraud, S. C.: Using boundary layer equilibrium to reduce uncertainties in transport models and CO_2 flux inversions, Atmos. Chem. Phys., 11, 9631–9641, doi:10.5194/acp-11-9631-2011, 2011.

Wunch, D., Wennberg, P. O., Toon, G. C., Keppel-Aleks, G., and Yavin, Y. G.: Emissions of greenhouse gases from a North American megacity, Geophys. Res. Lett., 36, L15810, doi:10.1029/2009gl039825, 2009.

Xiao, J. F., Zhuang, Q. L., Baldocchi, D. D., Law, B. E., Richardson, A. D., Chen, J. Q., Oren, R., Starr, G., Noormets, A., Ma, S. Y., Verma, S. B., Wharton, S., Wofsy, S. C., Bolstad, P. V., Burns, S. P., Cook, D. R., Curtis, P. S., Drake, B. G., Falk, M., Fischer, M. L., Foster, D. R., Gu, L. H., Hadley, J. L., Hollinger, D. Y., Katul, G. G., Litvak, M., Martin, T. A., Matamala, R., McNulty, S., Meyers, T. P., Monson, R. K., Munger, J. W., Oechel, W. C., Paw U, K. T.,

ACPD
14, 3231–3267, 2014

Schmid, H. P., Scott, R. L., Sun, G., Suyker, A. E., and Torn, M. S.: Estimation of net ecosystem carbon exchange for the conterminous United States by combining MODIS and AmeriFlux data, Agr. Forest Meteorol., 148, 1827–1847, doi:10.1016/j.agrformet.2008.06.015, 2008.

Yi, C., Davis, K. J., Bakwin, P. S., Berger, B. W., and Marr, L. C.: Influence of advection on measurements of the net ecosystem–atmosphere exchange of CO_2 from a very tall tower, J. Geophys. Res.-Atmos., 105, 9991–9999, doi:10.1029/2000jd900080, 2000.

Yi, C. X., Davis, K. J., Berger, B. W., and Bakwin, P. S.: Long-term observations of the dynamics of the continental planetary boundary layer, J. Atmos. Sci., 58, 1288–1299, doi:10.1175/1520-0469(2001)058<1288:Ltootd>2.0.Co;2, 2001.

Zhang, X.: Improving Regional-Scale Greenhouse Gas Inventories in an Agriculture-Dominated Landscape Using a Multi-Scale Approach, PhD Dissertation, Yale University, 2013.

Zhang, X., Lee, X., Griffis, T., Baker, J., Erickson, M., Hu, N., and Xiao, W.: The influence of plants on atmospheric methane in an agriculture-dominated landscape, Int. J. Biometeorol., 1–15, doi:10.1007/s00484-013-0662-y, 2013.

Zhang, X., Lee, X., Griffis, T., Andrews, A., Baker, J., Erickson, M., Hu, N., and Xiao, W.: Quantifying nitrous oxide fluxes on multiple spatial scales in the Upper Midwest, USA, in review, 2014.

Zhao, C. F., Andrews, A. E., Bianco, L., Eluszkiewicz, J., Hirsch, A., MacDonald, C., Nehrkorn, T., and Fischer, M. L.: Atmospheric inverse estimates of methane emissions from Central California, J. Geophys. Res.-Atmos., 114, D16302, doi:10.1029/2008jd011671, 2009.

Zhuang, Q. L., Lu, Y. Y., and Chen, M.: An inventory of global N_2O emissions from the soils of natural terrestrial ecosystems, Atmos. Environ., 47, 66–75, doi:10.1016/j.atmosenv.2011.11.036, 2012.

ACPD
14, 3231–3267, 2014

Table 1. Correlation coefficient and NSE (Nash–Sutcliffe efficiency) between EC flux and the other two methods. CT denotes CarbonTracker, and FA denotes the flux aggregation method.

Distance		5 km	10 k	20 k	50 k	100 km	200 km	300 km	600 km
CT	**NSE**	NA	NA	NA	NA	0.41	0.82	0.92	0.97
	r	NA	NA	NA	NA	0.96	0.97	0.98	0.99
FA	**NSE**	0.48	0.49	0.37	0.23	0.58	0.90	0.95	0.96
	r	0.98	0.98	0.98	0.98	0.98	0.98	0.98	0.98

ACPD
14, 3231–3267, 2014

Table 2. A summary of annual NEE estimated from different methods. NEE in the "Reference" column is from the study in Midwest US in recent years. Negative fluxes indicate carbon sink from the atmosphere and positive fluxes indicate carbon release to the atmosphere.

		This study ($g\,C\text{-}CO_2\,m^{-2}\,yr^{-1}$)	Reference ($g\,C\text{-}CO_2\,m^{-2}\,yr^{-1}$)
Tall tower eddy Covariance		-131 ± 35	120 ± 140 (1997–2004) (Ricciuto et al., 2010) 16 ± 19 (1997) (Davis et al., 2003) -71 (2000) (Helliker et al., 2004) 16 (1997) (Bakwin et al., 2004)
CarbonTracker		-54 ± 12	-58 (2000–2006) (Desai et al., 2010)
Equilibrium		46–74	-110 ± 14 (1997–2006) (Desai et al., 2010) -38 (2000) (Helliker et al., 2004) 79 (1997) (Bakwin et al., 2004)
Flux Aggregation		-130 ± 34	
	Corn	-599 ± 26	-466 ± 38 (2004–2007) (Hernandez-Ramirez et al., 2011) -576 ± 101 (1997–2002) (Hollinger et al., 2005)
	Soybean	10 ± 18	-13 ± 39 (2004–2007) (Hernandez-Ramirez et al., 2011) -32 ± 161 (1997–2002) (Hollinger et al., 2005)
	Grassland	-411 ± 10	-148 ± 116 (1997–1999) (Suyker et al., 2003)
	Forest	-227 ± 14	-137 ± 49 (1999–2001) (Schmid et al., 2003)
	Fossil fuel	124 ± 12	
Other methods			
Interannual Flux Tower Upscaling Experiment			-321 ± 13 (1997–2006) (Desai et al., 2010)
Mesoscale inverse modeling			-183 ± 35 (1997–2006) (Lauvaux et al., 2012)

ACPD
14, 3231–3267, 2014

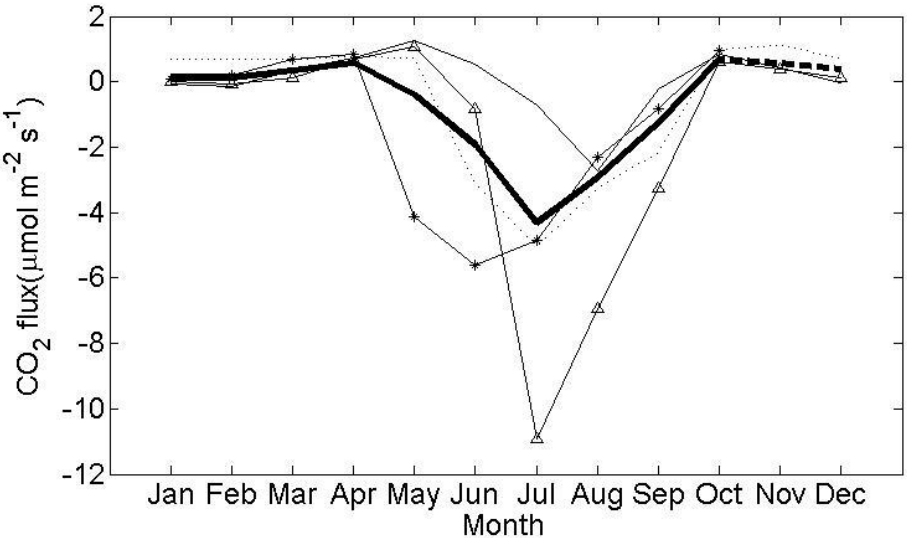

Fig. 1. The biogenic CO_2 flux (thick solid line) from the landscape around the tall tower, calculated from monthly averages of CO_2 flux from major land cover types. The fluxes for corn (solid line with triangles) and soybean (thin solid line) were measured with eddy covariance towers at the G21 and G19 site near the tall tower in Minnesota. The fluxes for forest (dotted line) and grassland (solid line with stars) were from UMBS and USIB2 AmeriFlux sites in North America.

ACPD
14, 3231–3267, 2014

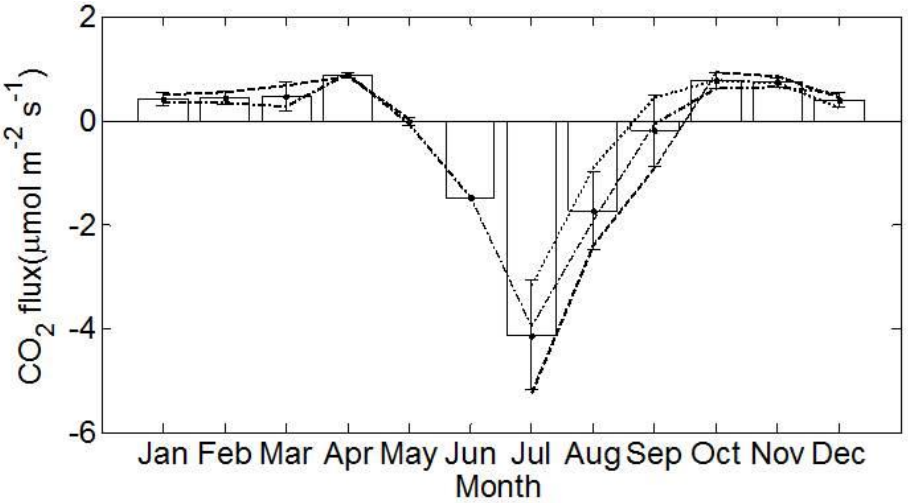

Fig. 2. Monthly averages of CO_2 flux in 2007 (dotted line), 2008 (dot-dashed line), and 2009 (dashed line) measured with EC on the tall tower. White bars are the mean monthly value from the available data during the three-year observation period. Error bars on the top of white bars are the standard deviation of the three-year measurements.

ACPD
14, 3231–3267, 2014

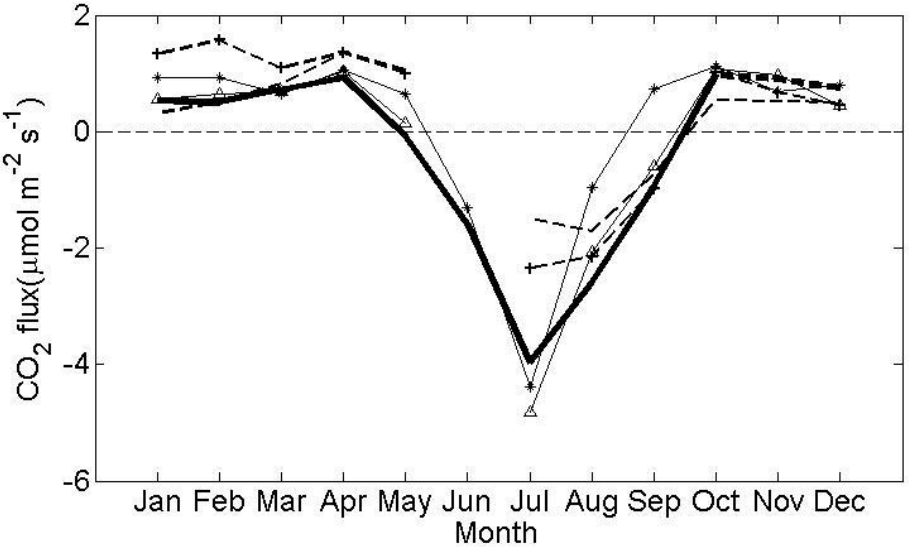

Fig. 3. Monthly CO_2 flux in 2009 estimated with flux aggregation (F_{FA}, thick solid line), eddy covariance method (F_{EC}, line with triangles), CarbonTracker (F_{CT}, line with stars), equilibrium method with H_2O as a tracer (F_{EH}, thin dashed line), and equilibrium method using NCEP reanalysis data (F_{EO}, thin dashed line with cross). The FA flux ended in October because the grassland data was missing in November and December. The missing FA flux was determined by assuming the missing grassland flux in November and December was the same as October flux (thick dashed line).

ACPD
14, 3231–3267, 2014

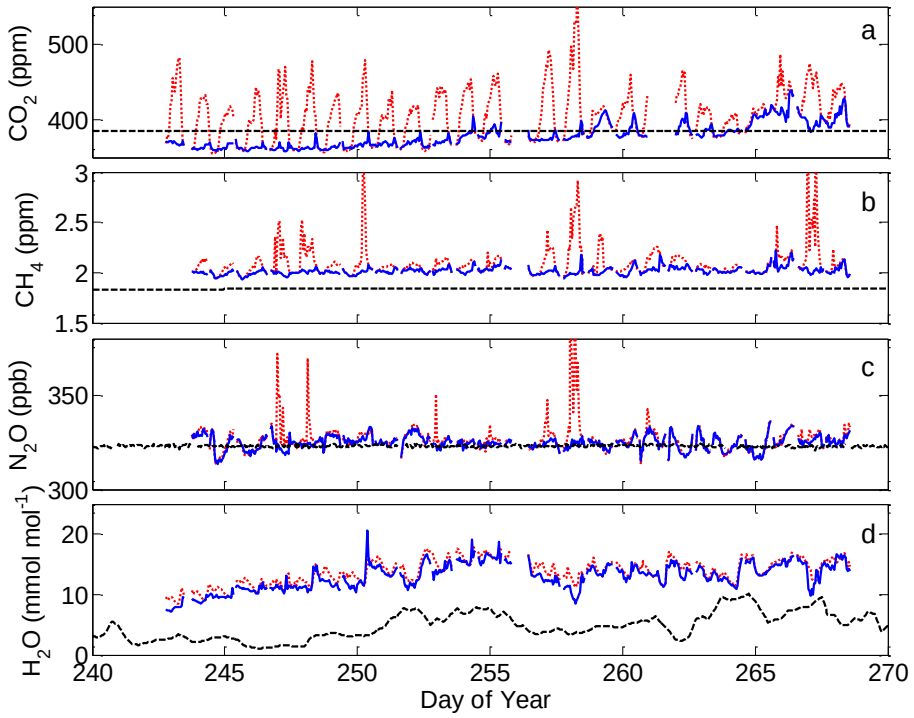

Fig. 4. Hourly averages of CO_2 **(a)**, CH_4 **(b)**, N_2O **(c)**, and H_2O **(d)** mixing ratio during the observation period from DOY 243 to DOY 269, 2009. Blue solid line – mixing ratio on 200 m. Red dotted line – mixing ratio on 3 m. Black dashed line – mixing ratio at Niwot Ridge site.

ACPD
14, 3231–3267, 2014

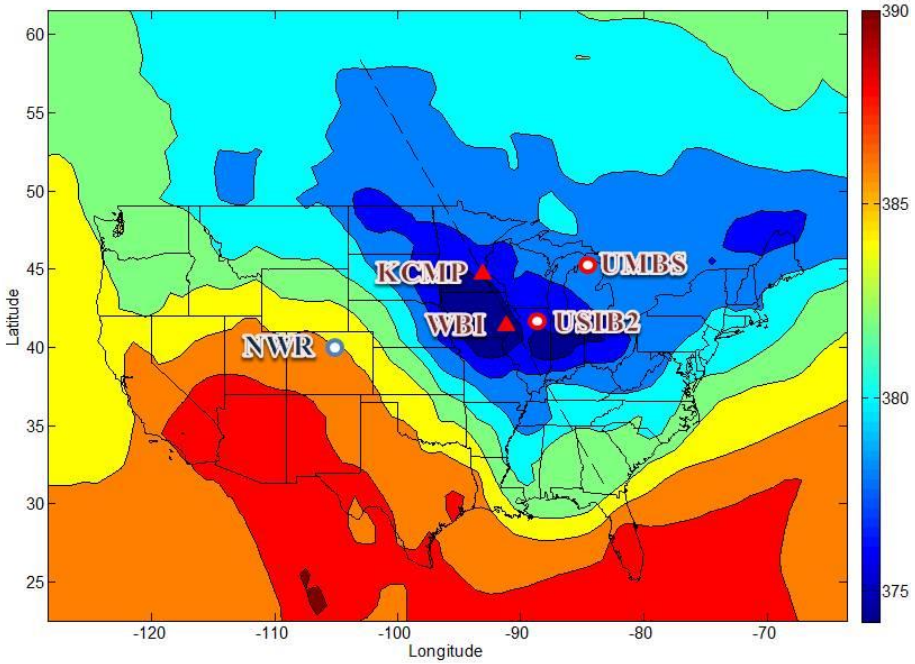

Fig. 5. CO_2 concentration averaged from land surface to 1274 m according to the CarbonTracker 3-D CO_2 concentration product in July 2009. Dashed line – prevailing wind direction in July from northwest to southeast. Red triangle – our tall tower site (KCMP) and WBI tower obserservotory operated by NOAA. Red circle – Ameriflux sites. Blue circle – background observation site. The color scale is the CO_2 concentration in ppm. The resolution of the concentration data is 1° by 1°.

ACPD
14, 3231–3267, 2014